

# Graft polymerisation of acrylamide onto PCL film by electron beam pre-irradiation in air or argon. Morphology in the final grafted state

T. Lindberg, A. Wirsén, A.-C. Albertsson\*

*Department of Polymer Technology, The Royal Institute of Technology, Stockholm, SE-100 44, Sweden*

Received 16 April 1999; received in revised form 6 July 1999; accepted 29 July 1999

## Abstract

Poly( $\epsilon$ -caprolactone) has been graft polymerised to final graft yields with acrylamide (AAm) as monomer in an aqueous solution by the pre-irradiation method. The synthesis of the samples obtained, pre-irradiated in air or argon atmosphere, was controlled by dose and concentration of inhibitor, provided as Mohr's salt, in the ranges from 2.5 to 10 Mrad and from 0.005 to 0.500 wt%, respectively. Final graft yields and lateral dimensions in swollen condition ranged from 70 to 3400 wt%, and from  $23 \times 30$  to  $89 \times 94$  mm<sup>2</sup>, respectively, as atmosphere during irradiation, dose and concentration of inhibitor were altered. These properties gave values in crystallinity extending from 4 to 57 wt%. Samples pre-irradiated in air and subsequently graft polymerised yielded higher values of crystallinity in the entire range of dose and concentration of inhibitor. At low concentration of inhibitor, final graft yield and lateral dimension for samples pre-irradiated in air had considerably larger values while the final graft yield and lateral dimension of samples pre-irradiated in argon had slightly larger values at high concentration of inhibitor. The initial biaxial morphology of the PCL film was continuously transformed into a uniform morphology, which was reached at a final graft yield of approximately 800 wt%. © 2000 Elsevier Science Ltd. All rights reserved.

*Keywords:* Poly( $\epsilon$ -caprolactone); Acrylamide; Graft polymerisation

## 1. Introduction

Heterogeneous graft polymerisation of polymers in their solid state with an aqueous monomer solution is a versatile way of hydrophilisation [1–5]. This may be accomplished by initial introduction of free radicals within the trunk polymer using high energy irradiation [6–8] followed by exposure to monomer in a separate subsequent graft polymerisation step. High-energy irradiation of polymers generates molecular alterations which depend on the chemical structure and morphology, as well as on irradiation conditions (atmosphere, temperature, dose rate, dose). Particularly for polyethylenes (PE), the effects of the  $\gamma$  and EB irradiation have been studied extensively [9–11]. To summarise, irradiation of PE primarily generates alkyl, allyl and polyenyl radicals which upon exposure to air initially will form peroxy radicals [9]. The radicals formed in poly( $\epsilon$ -caprolactone), PCL, during EB irradiation in argon atmosphere are predominantly secondary alkylether radicals whereas in air atmosphere peroxy radicals are formed additionally [12].

PCL is a semicrystalline polymer with a crystallinity of ~50 wt%, having a melting temperature of 60°C and a glass

transition temperature of  $-60^\circ\text{C}$  [13]. The conformation and the unit cell of PCL resemble those of PE [14] although the molecular structure in PCL contains an ester group instead of a methylene sequence, see Fig. 1.

PCL is usually produced by ring opening polymerisation, creating linear molecules while commercial PE to a widely varying extent contains chain branches. The differences mentioned generate different physical properties between the polymers regarding glass transition temperatures,  $-100$  and  $-60^\circ\text{C}$  [13,15], melting temperatures, 125 and  $60^\circ\text{C}$  [15,13] and heats of fusion at equilibrium, 293 and  $139 \text{ J g}^{-1}$  [15,16], for PE and PCL, respectively.

Upon exposure of the irradiated solid trunk polymer to the monomer containing phase, grafting will proceed from the surface towards the interior of the solid phase. The progress of graft polymerisation is commonly characterised by the increase in graft yield where the graft yield is defined as the percentage increase in dry weight in relation to the ungrafted trunk polymer. The characteristic evolution of the graft yield with time for PCL pre-irradiated to 2.5, 5 and 10 Mrad in air at a specific inhibitor concentration (Mohr's salt) is shown in Fig. 2. Three apparent stages occur as time is increased: an induction stage, a seemingly linear stage and a final graft yield ( $G_f$ ), also called the saturation graft yield.

\* Corresponding author. Tel.: +46-8-790-6000; fax: +46-8-10-0775.

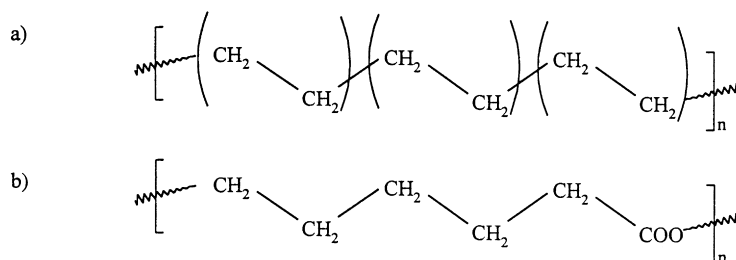


Fig. 1. Molecular structures of (a) PE and (b) PCL.

In general,  $G_f$  for an irradiated polymer during graft polymerisation is in the main governed by the concentration of the grafting monomer, the temperature, the dose and the addition of inhibitor [2,7]. The latter is added to prevent homopolymerisation which may be extensive due to chain transfer to monomer or, when hydroperoxides are present, initiation by hydroxy radicals. Although the inhibitor is mainly added to suppress the formation of homopolymer, it will also influence the graft yield which is seen as a decrease in  $G_f$  with inhibitor concentration. Acrylamide (AAM) which is chosen as the monomer to be grafted in this study is a highly reactive and hydrophilic monomer. After the graft polymerisation it can be further derivatised for coupling reactions [17].

The aim of this work is to prepare samples of the grafting system P(CL-g-AAM) in their final grafted state. The morphology of the samples is investigated as the atmosphere during irradiation (air or argon) the dose and concentration of inhibitor are altered. Moreover, the dimensional expansion of the grafted samples in the swollen state for various doses and inhibitor concentrations in each atmosphere is analysed. The proposed approach gives the opportunity to design materials with controlled graft yield and morphology.

## 2. Experimental

### 2.1. Materials

Films of PCL, having a film thickness of  $30 \pm 2 \mu\text{m}$ , were prepared by film blow moulding of granules of Tone 787, free from additives, kindly provided by the Union Carbide Company. The molecular weights of virgin PCL were  $\bar{M}_n \approx 130\,000 \text{ g mol}^{-1}$  and  $\bar{M}_w \approx 205\,000 \text{ g mol}^{-1}$ , as measured by SEC calibrated against PS standards. The crystallinity ( $w_c$ ) was  $50 \pm 3$  and  $56 \pm 2 \text{ wt}\%$  as measured by DSC and X-ray diffraction (XRD), respectively. Acrylamide (AAM), (Pharmacia LKB 80-1128-10) and Mohr's salt  $[(\text{NH}_4)_2\text{Fe}(\text{SO}_4)_2 \cdot 6\text{H}_2\text{O}]$  (Merck 3792) were used as received.

### 2.2. Irradiation and grafting

The graft polymerisation has been reported earlier [18]. In short, film samples of PCL ( $2 \times 2 \text{ cm}^2$ ) were pre-irradiated

in air or argon atmosphere in the dose range of 2.5–10 Mrad with a dose rate of  $0.8 \text{ Mrad min}^{-1}$  and an electron energy of 6.5 MeV. The pre-irradiated samples were stored in liquid nitrogen prior to the graft polymerisation. The samples were transformed to an aqueous solution of acrylamide monomer where the temperature and the concentration of monomer were kept constant at  $35^\circ\text{C}$  and 20 wt%, respectively; Mohr's salt was provided as inhibitor in the range of 0.005–0.500 wt%. The grafting solutions were purged with argon during 15 min before insertion of the pre-irradiated film samples. All graft polymerised samples were ensured to reach the final grafted state by using a polymerisation time ( $60 \pm 10 \text{ min}$ ) well above the time needed to obtain this state [19].

### 2.3. Swelling dimensions

The lateral dimensions of the swollen samples as obtained in the grafting were measured in swollen condition with a millimetre scale. All samples measured had rectangular shapes. The dimensions are designated width ( $W$ ) and length ( $L$ ) where the width was taken as the largest value.

### 2.4. X-ray diffraction

Measurements were carried out on a Philips generator

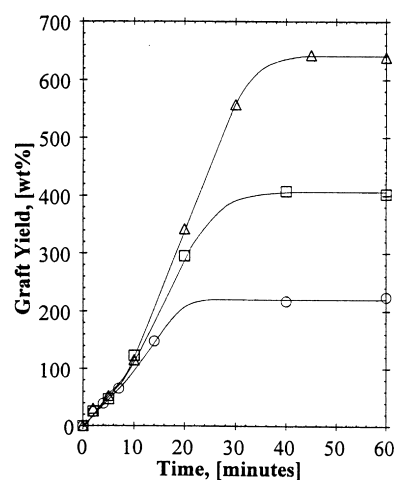


Fig. 2. Graft polymerisation with time for P(CL-g-AAM) pre-irradiated in air to 2.5 Mrad (circles), 5 Mrad (boxes) and 10 Mrad (triangles) at  $35^\circ\text{C}$ , 20 wt% AAM and 0.050 wt% Mohr's salt. Data from Ref. [19].

Table 1  
Average molecular weights (from Ref. [12]) and crystallinities as measured by XRD and DSC for PCL irradiated in air or argon

Dose (Mrad)	$\bar{M}_n \times 10^{-3}$ (g mol <sup>-1</sup> )		$\bar{M}_w \times 10^{-3}$ (g mol <sup>-1</sup> )		$w_c^{\text{XRD}}$ (wt%)		$w_c^{\text{DSC}}$ , (wt%)	
	130		205		56 ± 2		50 ± 3	
Irradiation in	Air	Argon	Air	Argon	Air	Argon	Air	Argon
2.5	102	88	170	165	57	50	54	48
5	80	75	150	148	57	49	55	48
7.5	–	–	–	–	58	50	56	47
10	56	47	112	101	60	51	58	49

PW 1830, nickel filtered CuK $\alpha$ -radiation ( $\lambda = 1.542 \text{ \AA}$ ), with a Warhus camera under vacuum, and an image analysis system. The diffractograms obtained in the image analysis system, were converted from light to intensity and analysed, assuming a linear Lorenz–Gaussian relation [20].

The intensities were determined according to the procedure proposed by Baltá-Calleja and Vonk [21]. Corrections were made according to the procedure proposed by Kakudo and Kasai [22], added by the correction for variation in absorption with graft yield.

As a measure of the crystallinity of the samples, we used the expression

$$w_c^{\text{XRD}} = \frac{I_c^{110} + I_c^{111} + I_c^{200}}{I_a + I_c^{110} + I_c^{111} + I_c^{200}} \quad (1)$$

where  $I_a$  and  $I_c^{hkl}$  are the areas under the amorphous halo and the  $hkl$ -reflections, respectively. PCL gives reflections at  $2\theta = 21.6^\circ(110)$ ,  $2\theta = 24.0^\circ(200)$  and  $2\theta = 22.2^\circ(111)$  [14]. The major contribution to the crystallinity (>95%) originates from the reflections from the planes (110) and (200).

In order to obtain  $w_c^{\text{XRD}}$  for the PCL backbone in grafted samples, a polyacrylamide correction was introduced for the contribution of PAAm to the amorphous halo. This was obtained from diffractograms of random oriented film samples made by stacking ungrafted PCL films with varying amounts of PAAm films, simulating different graft yields. Since  $w_c^{\text{XRD}}$ , which only refers to PCL, was kept unchanged, an internal correction for the contribution of PAAm was obtained as a function of graft yield.

### 2.5. Differential scanning calorimetry

Melting endotherms were measured on a Perkin–Elmer DSC-7 calorimeter with sample weights of  $6 \pm 4$  mg, depending on the graft yield, and a heating rate of  $20^\circ\text{C min}^{-1}$ . The instrument was calibrated with indium ( $T_m = 429.8 \text{ K}$ ,  $\Delta H_f = 28.46 \text{ J g}^{-1}$ ). Samples were preheated to  $80^\circ\text{C}$  and cooled at  $20^\circ\text{C min}^{-1}$  to  $-60^\circ\text{C}$  and kept at that temperature for 5 min after which they were heated again to  $80^\circ\text{C}$  at  $20^\circ\text{C min}^{-1}$ ; during the latter scan the heat of fusion was recorded. In evaluating the crystallinity it was assumed that the only contribution for the polyacrylamide grafted samples originated from the crystallites remaining in the trunk polymer. According to separate

measurements by DSC and XRD, PAAm is essentially amorphous having a  $T_g$  of 468 K [23] which is well above the melting endotherm for PCL.

The crystallinity was evaluated according to

$$w'_c = \frac{\Delta H_f}{\Delta H_{T_m}^0} \quad (2)$$

where  $\Delta H_f$  is the value of the measured heat of fusion and  $\Delta H_{T_m}^0$  is the equilibrium heat of fusion ( $139.5 \text{ J g}^{-1}$ ) which was obtained from Crezcenzi et al. [16].

The crystallinity for grafted samples was corrected for graft yield (GY) according to

$$w_c^{\text{DSC}} = w'_c \left( 1 + \frac{\text{GY}(\%)}{100} \right) \quad (3)$$

where  $w'_c$  was obtained from formula (2).

### 2.6. Scanning electron microscopy

The thickness in dry condition was measured with scanning electron microscopy (SEM). The specimen was prepared in liquid nitrogen and the sputtering material was applied from an Au/Pd cathode to a thickness of approximately 10 nm. Microscopy investigation was performed on a Jeol SEM-5400.

### 2.7. Environmental scanning electron microscopy

The thickness in swollen condition was obtained with environmental scanning electron microscopy (ESEM). Microscopy studies were performed on an ElectroScan ESEM-2020 at STFI, Stockholm, Sweden. The microscope operating conditions were an accelerating voltage of 15 kV, a working distance of 8.3  $\mu\text{m}$ , a sample chamber pressure of 6 Torr and a test piece temperature of  $-5^\circ\text{C}$ .

## 3. Results and discussion

### 3.1. Effect of irradiation

In Table 1 the crystallinities as measured by XRD and DSC for PCL irradiated in air or argon are displayed. The corresponding molecular weights, originating from Ref. [12], are also presented.

The virgin PCL has a crystallinity of  $56 \pm 2$  and  $50 \pm$

Table 2

Field graft yields ( $G_f$ ), lateral dimensions and crystallinities ( $w_c$ ) as measured by XRD and DSC for the system P(CL-g-AAm) pre-irradiated in air and graft polymerised at 35°C with a concentration of 20% AAam at various irradiation doses and concentrations of Mohr's salt

Dose (Mrad)	[Mohr's salt] (wt%)	$G_f$ (wt%)	Length (mm)	Width (mm)	$w_c^{\text{XRD}}$ (wt%)	$w_c^{\text{DSC}}$ (wt%)
2.5	0.500	73 ± 6	23 ± 0	30 ± 1	57	45
2.5	0.250	100 ± 3	24 ± 0	32 ± 1	48	40
2.5	0.100	153 ± 8	27 ± 1	34 ± 1	45	36
2.5	0.050	223 ± 9	32 ± 1	38 ± 1	43	30
2.5	0.025	389 ± 21	41 ± 1	44 ± 0	33	24
2.5	0.010	805 ± 80	53 ± 1	54 ± 2	20	17
2.5	0.005	1270 ± 97	62 ± 2	66 ± 2	19	14
5	0.500	112 ± 0	25 ± 1	33 ± 0	52	42
5	0.250	149 ± 1	28 ± 2	34 ± 1	48	36
5	0.100	240 ± 12	32 ± 1	38 ± 1	46	32
5	0.050	358 ± 7	39 ± 1	43 ± 2	39	27
5	0.025	702 ± 24	52 ± 3	53 ± 2	32	22
5	0.010	1412 ± 55	65 ± 3	70 ± 4	25	19
5	0.005	1856 ± 247	73 ± 3	78 ± 4	17	17
7.5	0.500	121 ± 7	26 ± 1	34 ± 1	57	40
7.5	0.250	171 ± 5	28 ± 0	35 ± 0	55	35
7.5	0.100	300 ± 2	34 ± 1	40 ± 1	34	31
7.5	0.050	512 ± 18	46 ± 2	49 ± 1	28	27
7.5	0.025	914 ± 15	56 ± 1	57 ± 1	27	21
7.5	0.010	1900 ± 8	74 ± 1	77 ± 1	15	17
7.5	0.005	2885 ± 23	88 ± 4	91 ± 2	12	15
10	0.500	137 ± 5	25 ± 1	33 ± 1	57	43
10	0.250	199 ± 7	30 ± 1	34 ± 2	48	40
10	0.100	353 ± 11	37 ± 1	42 ± 1	44	34
10	0.050	627 ± 57	49 ± 1	51 ± 1	32	31
10	0.025	1018 ± 69	59 ± 2	60 ± 2	24	24
10	0.010	2266 ± 81	79 ± 2	84 ± 4	18	19
10	0.005	3361 ± 82	89 ± 1	94 ± 1	17	15

3 wt% as measured by XRD and DSC, respectively. The  $w_c^{\text{DSC}}$  data refer to the second run of the DSC analysis and thus depend on re-crystallisation [24–26]. This is seen for the virgin PCL, which has a higher crystallinity when measured by XRD as compared with DSC. After irradiation in air up to 10 Mrad this difference decreases while there is a slight increase with dose to 60 and 58 wt%. This is accompanied by a decrease in  $\bar{M}_n$  as well as  $\bar{M}_w$ , implying that chain scission is the net effect in this dose range. This favours re-crystallisation even in the solid state which has been verified in several investigations on polyethylenes after irradiation in air [27–29]. As seen in Table 1 the crystallinity values upon irradiation in argon differ significantly from those obtained in air whereas the XRD and DSC data are quite similar and constant throughout the dose range, although on a lower level than for irradiation in air, i.e. 50 wt% for XRD and 48 wt% for DSC. Since XRD is measured on the unperturbed samples, the XRD data indicate an actual decrease in crystallinity from 56 wt% for unirradiated PCL as compared to 50 wt% for 2.5–10 Mrad in argon. It has been shown for other semicrystalline polymers, including polyethylenes irradiated under inert conditions that crosslinking occurs at the chain folds and in the transient phase at the crystallite surfaces [30,31]. Since PCL and PE have similar folding characteristics [25,32], it seems plausible that the molecular conformations at the lamellae

surfaces are similar in spite of the differences in chemical structure. The crosslinking localised to the crystallite surfaces and at lamellae folds may prevent further changes in crystallinity but the decrease in crystallinity from 0 to 2.5 Mrad as obtained by XRD indicates an initial deterioration of the crystallites which is not seen for the same irradiation in air.

### 3.2. Graft polymerised samples

The data obtained for PCL samples pre-irradiated in air and argon and subsequently graft polymerised to their final grafted state, are compiled in Tables 2 and 3, respectively. Values of  $G_f$  and lateral dimensions are given as mean values with the corresponding standard deviations obtained from two or more samples grafted at the respective combination of dose and concentration of inhibitor. The crystallinity data, as obtained by XRD and DSC, are from a sample with a  $G_f$  close to the mean value of each respective  $G_f$ . As mentioned in Section 2, the crystallinity data— $w_c^{\text{XRD}}$  and  $w_c^{\text{DSC}}$ —refer only to the PCL core of the grafted samples, since corrections were made for the dilution effect of the grafting.

As seen in Table 2, variations of dose and concentration of inhibitor in the ranges from 2.5 to 10 Mrad and from 0.005 to 0.500 wt%, respectively, give samples with  $G_f$

Table 3

Final graft yields ( $G_f$ ), lateral dimensions and crystallinities ( $w_c$ ) as measured by XRD and DSC for the system P(CL-g-AAm) pre-irradiated in argon and graft polymerised at 35°C with a concentration of 20 wt% AAam at various irradiation doses and concentrations of Mohr's salt

Dose (Mrad)	[Mohr's salt] (wt%)	$G_f$ (wt%)	Length (mm)	Width (mm)	$w_c^{XRD}$ (wt%)	$w_c^{DSC}$ (wt%)
2.5	0.500	94 ± 4	23 ± 0	31 ± 1	48	36
2.5	0.050	257 ± 46	36 ± 1	38 ± 1	29	25
2.5	0.005	938 ± 98	56 ± 2	58 ± 3	10	8
5	0.500	123 ± 6	23 ± 1	31 ± 2	45	35
5	0.250	161 ± 5	27 ± 1	34 ± 0	43	32
5	0.100	251 ± 21	32 ± 1	38 ± 1	31	30
5	0.050	360 ± 41	37 ± 0	42 ± 1	28	23
5	0.025	556 ± 28	46 ± 1	48 ± 1	18	15
5	0.010	765 ± 49	53 ± 2	54 ± 1	14	11
5	0.005	1126 ± 88	57 ± 2	61 ± 2	7	5
7.5	0.500	132 ± 7	25 ± 0	32 ± 1	43	32
7.5	0.050	462 ± 8	42 ± 0	47 ± 4	24	19
7.5	0.005	1366 ± 618	63 ± 9	68 ± 11	8	5
10.0	0.500	139 ± 21	26 ± 1	33 ± 1	40	31
10.0	0.050	528 ± 18	45 ± 1	47 ± 1	20	15
10.0	0.005	1463 ± 316	65 ± 6	72 ± 7	5	4

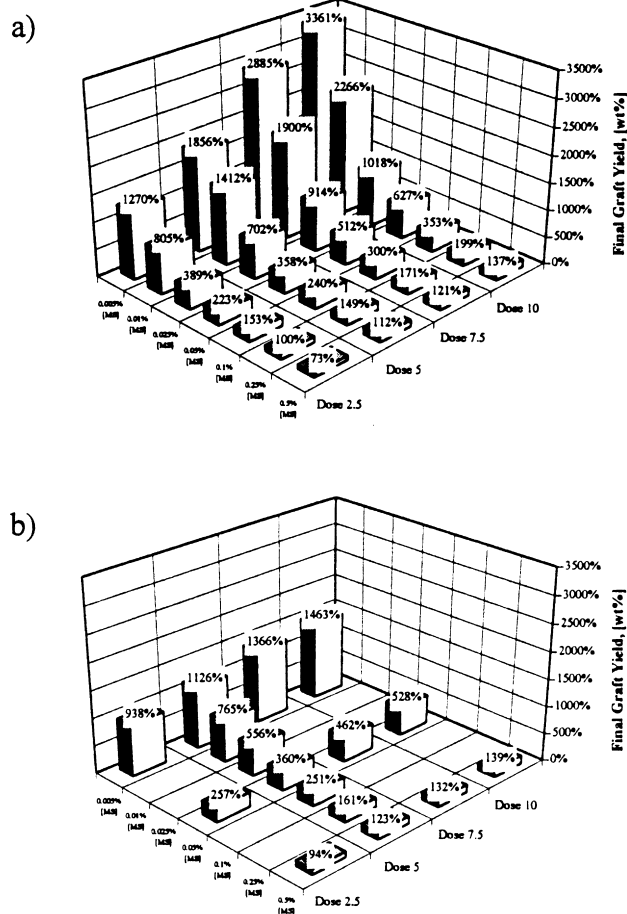


Fig. 3. Final graft yield of P(CL-g-AAm) pre-irradiated in (a) air or (b) argon as a function of dose and concentration of Mohr's salt [MS]. Conditions as in Tables 2 and 3.

ranging from ~70 to ~3400 wt% for samples pre-irradiated in air; the higher  $G_f$  are obtained at high doses and low concentrations of inhibitor, i.e. Mohr's salt. Accordingly, the lateral dimensions of samples in the swollen state vary within broad limits:  $23 \times 30$  to  $89 \times 94$  mm<sup>2</sup> reflecting the respective final degrees of grafting,  $G_f$ . The crystallinity also changes between 12 and 57 wt%, and between 14 and 45 wt%, as measured by XRD and DSC, respectively; however, in reverse order to the graft yield and swelling data.

In Table 3 the same properties as in Table 2— $G_f$ , lateral dimensions and  $w_c$ —as a function of dose and inhibitor concentration are given for samples pre-irradiated in argon and subsequently graft polymerised. The same principal dependencies for  $G_f$  on irradiation dose and inhibitor concentration are observed although all properties show lower variations. Anyhow, the variations are significant:  $G_f$  ranges from ~90 to ~1500 wt%, the lateral dimensions range from  $23 \times 31$  to  $65 \times 72$  mm<sup>2</sup> and the crystallinities extend from 5 to 48 wt% and from 4 to 36 wt% as detected by XRD and DSC, respectively.

### 3.3. Graft yields

In Fig. 3(a) and (b),  $G_f$  for samples pre-irradiated in air or argon, as a function of dose and concentration of inhibitor, are shown in three-dimensional diagrams. To be noted, the inhibitor concentrations are represented at equal distances in the grid regardless of internal proportions. The actual dependence of  $G_f$  on linear inhibitor concentration is shown more accurately in Figs. 4(b) and 6(b). However, the three dimensional diagrams, as presented here, are shown with the intention to visualise differences in  $G_f$  for irradiation in air and argon.

As seen in Fig. 3(a) and (b), the highest as well as the

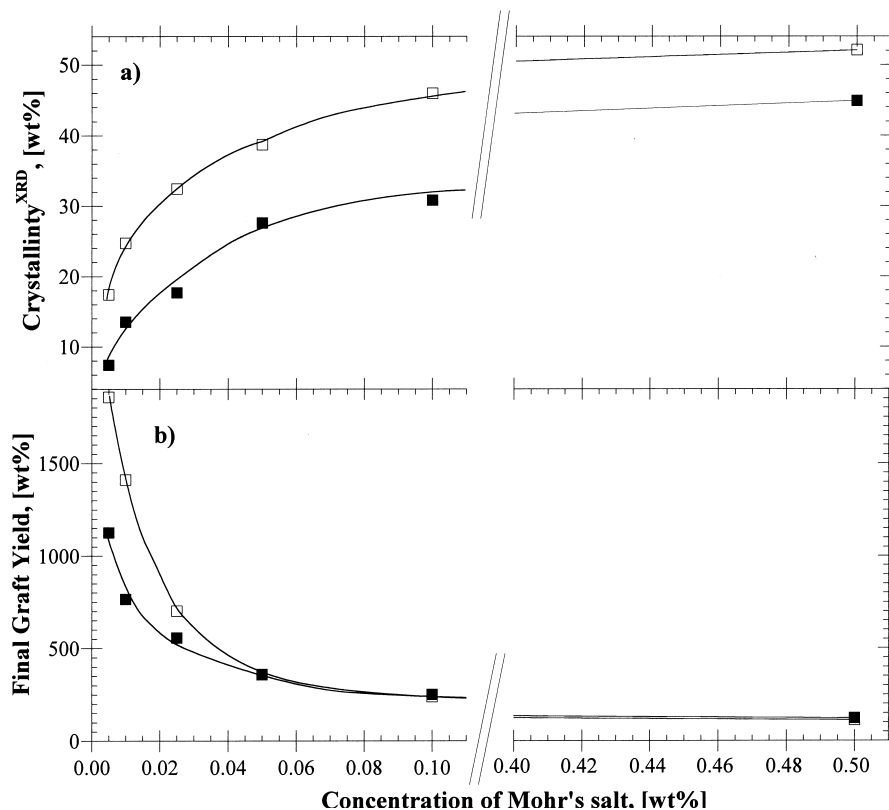


Fig. 4. Crystallinity (boxes), as measured by XRD, and final graft yield (circles) as a function of concentration of Mohr's salt for P(CL-g-AAm) pre-irradiated to 5 Mrad in air (open symbols) and in argon (closed symbols). Conditions as in Tables 2 and 3.

lowest  $G_f$  values belong to the samples pre-irradiated in air. Below an inhibitor concentration of 0.05 wt% these  $G_f$  data are higher and also their increase in  $G_f$  as the inhibitor concentration is further lowered, is much faster compared to pre-irradiation in argon. To the contrary for increasing concentration of inhibitor, there is an area from 0.05 wt% at 2.5 Mrad to 0.5 wt% at 10 Mrad where  $G_f$  is higher for pre-irradiation in argon. Although the  $G_f$  values are much smaller in this region this difference is consistent. In the mid region—0.05 wt% inhibitor and 5 Mrad—the  $G_f$  values seem identical; 358 and 360 wt% for air and argon samples, respectively. This is in agreement with an earlier investigation using the same grafting conditions [19]. As is obvious from the present investigation, this is not a general performance but limited to a transition zone between high and low  $G_f$  values. In Tables 2 and 3 also the crystallinity data as measured by XRD and DSC are given. In all cases there is a decline in crystallinity in the PCL core with increasing  $G_f$ . Also in this case, the DSC data are from the second run and consistently lower than the XRD data, as expected from re-crystallisation effects.

### 3.4. Effect of atmosphere

When comparing Tables 2 and 3 it is evident that the crystallinity remaining in the PCL core of the grafted samples is consistently lower for pre-irradiation in argon.

This is also shown in Fig. 4a and b where the crystallinity, as measured by XRD, and  $G_f$  for 5 Mrad in air or argon are plotted versus concentration of inhibitor.

For both atmospheres there is an inverted relation between  $G_f$  and crystallinity. As the inhibitor concentration is increased  $G_f$  decreases and crystallinity increases with the highest changes in the low concentration range. At higher inhibitor concentrations the curves level off, approaching almost constant values. The difference between the crystallinity curves for air and argon (Fig. 4a) has no correspondence in  $G_f$  curves (Fig. 4b). Only for inhibitor concentrations below 0.05 wt% where both  $G_f$  curves increase steeply as the inhibitor concentration is lowered there is a clear divergence in that  $G_f$  for air increases more than for argon.

### 3.5. Effect of dose and inhibitor

The results of the final graft yield ( $G_f$ ) as a function of dose at various inhibitor concentrations of samples pre-irradiated in air, are shown in a logarithmic diagram in Fig. 5, and in a linear diagram in Fig. 6.

The final graft yield ( $G_f$ ) represents the total grafted mass, which is possible to obtain under each specific grafting condition. It is constituted by the number of graft polymerised chains and their average molecular weight from the beginning of the grafting reaction until it spontaneously

ceases by exhaustion of initiating sites. In principle in homogeneous systems  $G_f$  would be directly correlated to the amount of initiating radicals and the rates of the graft initiation, propagation and termination reactions. In addition grafting in a heterogeneous system involves transport phenomena across moving phase boundaries where permeation and amount of reactants may change during the grafting. Although the irradiation dose has a direct correlation to the radicals generated in the trunk polymer their decay, accessibility and the monomer supply will have impacts on the order of dependence between  $G_f$  and the irradiation dose ( $D$ ). In radiation induced heterogeneous grafting, an inhibitor such as  $\text{Fe}^{2+}$  in the form of Mohr's salt, is added to suppress homopolymerisation in the liquid phase. Since  $G_f$  is strongly dependent on the inhibitor concentration it may in principle terminate grafted chain radicals as well as primary radicals in the trunk polymer. The latter case would be expected to occur at high concentrations of inhibitor.

In Fig. 5 the final graft yield ( $G_f$ ) is plotted versus the pre-irradiation dose ( $D$ ) in logarithmic diagrams for various inhibitor concentrations. From the slopes in Fig. 5 the dose exponents  $G_f$  for samples pre-irradiated in air at the different inhibitor concentrations are obtained. The identical analysis was made with the samples pre-irradiated in argon. Both analyses are summarised in Table 4.

For samples pre-irradiated in air, the dose exponent is constant with an average of 0.73 for an inhibitor concentration from 0.005 to 0.050 wt%. Above the latter concentration, the exponent declines as the concentration of inhibitor is increased. The uniform dose exponent for inhibitor concentrations at 0.050 wt% and below is connected with high and rapidly increasing  $G_f$  as discussed previously in conjunction with Fig. 3 and Fig. 4. In this range we propose that the inhibitor predominantly terminates the graft propagation. In an earlier investigation on pre-irradiation of acrylamide onto LLDPE, which shows very similar behaviour, it was concluded that  $G_f$  varied as would the average molecular weight upon monomolecular chain termination by  $\text{Fe}^{2+}$ , for the same concentration range as in the present system [33]. For inhibitor concentrations above 0.050 wt%, the dose exponent gradually decreases to about 0.45 at 0.500 wt% which might indicate an additional extinction of primary radicals. As was previously shown in Fig. 4b for  $G_f$  versus inhibitor concentration for a dose of 5 Mrad,  $G_f$  becomes seemingly independent of the inhibitor concentration above 0.100–0.250 wt% where it approaches a finite value above zero. This may imply that a minimum chain length is required for termination by the inhibitor since  $\text{Fe}^{2+}$  with counter-ions would not penetrate into the grafting zone as well as the acrylamide monomer [33,34]. Further, even at 0.500 wt% of inhibitor and a 20 wt% monomer solution,  $\text{Fe}^{2+}$  is outnumbered by acrylamide monomer by a molar ratio of 1 to 220. However, at this amount of inhibitor the frequent chain termination alone would lower the grafting rate, allowing a higher proportion of the primary radicals to

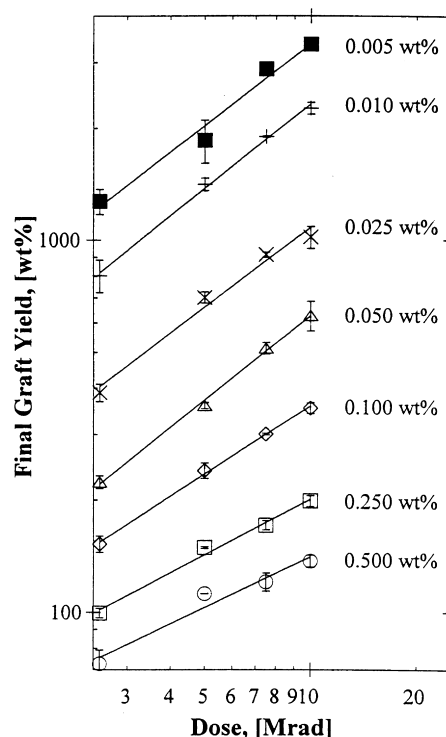


Fig. 5. Final graft yield for P(CL-g-AAm) pre-irradiated in air as a function of dose at varying inhibitor concentrations. From bottom to top: 0.500 wt% (open circles), 0.250 wt% (open boxes), 0.100 wt% (open diamonds), 0.050 wt% (open triangles), 0.025 wt% (tilted crosses), 0.010 wt% (crosses) and 0.005 wt% (crossed boxes). Standard deviations are indicated as vertical bars. Conditions as in Tables 2 and 3.

decay before the initiation. Nevertheless, whether initiating radicals would be lost by reduced grafting rate or by direct termination by inhibitor, the result would be a reduction in the dose exponent for  $G_f$  in both cases.

As seen in Fig. 6, the crystallinity and  $G_f$  curves for samples pre-irradiated in air show the same inhibitor dependence as discussed in Fig. 4. Although there is a scatter in the crystallinity data in Fig. 6 the crystallinity decreases with dose particularly below an inhibitor concentration of 0.100 wt%. This corresponds to an increase in  $G_f$  as the dose is raised. Also for  $G_f$  the effect is higher for inhibitor concentrations below 0.100 wt%, however the dose dependence is reversed; an increase in  $G_f$  with dose corresponds to a decrease in crystallinity. The concentration of radicals formed has been reported to be proportional to the dose in the case of PE [35]. However,  $G_f$  is not directly proportional to the dose, as is evident from the dose exponent in Table 4. A higher dose requires longer time during irradiation since the dose rate is constant. Thus at ambient temperature a larger portion of the total amount of free radicals will decay as the dose is raised. Furthermore, at high doses a saturation effect may be reached due to recombination, which will give an upper limit for the radical concentration. At inhibitor concentrations of 0.050 and 0.005 wt%,  $G_f$  is increased by factors  $\sim 2.8$  and  $\sim 2.7$ , respectively, as the

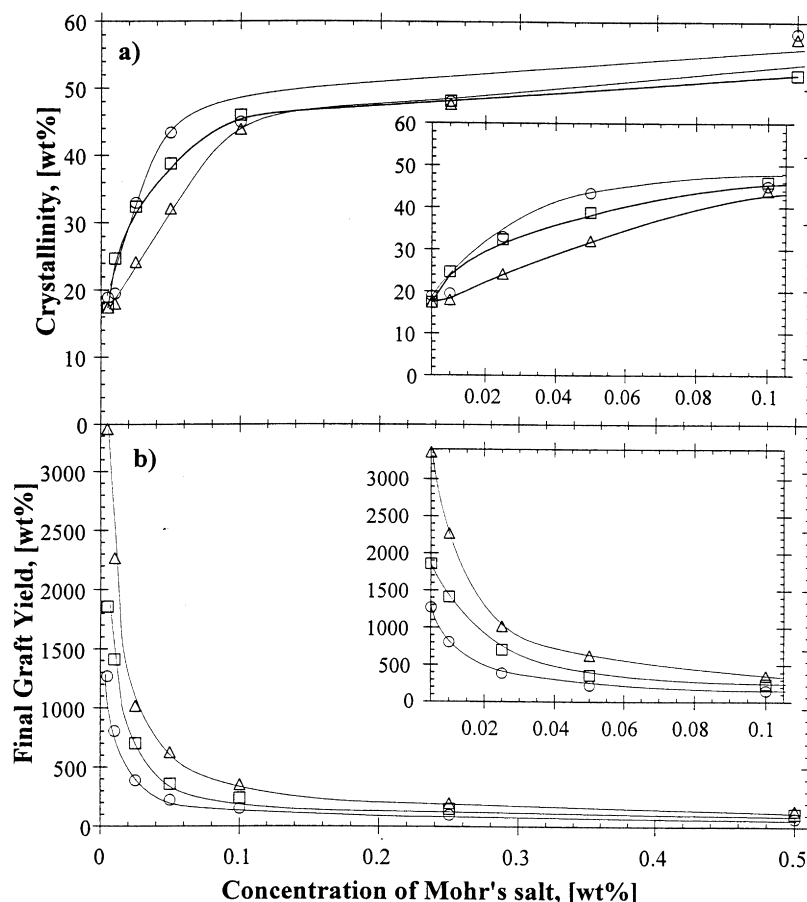


Fig. 6. Crystallinity as measured by XRD and final graft yield as a function of concentration of Mohr's salt for P(CL-g-AAm) pre-irradiated in air to 2.5 Mrad (circles), 5 Mrad (boxes) and 10 Mrad (triangles). Conditions as in Table 2.

dose is raised from 2.5 to 10 Mrad but at an inhibitor concentration of 0.500 wt%  $G_f$  is increased  $\sim 1.8$  times for the same dose increase, see Table 2 and Fig. 6. The significantly lower increase in  $G_f$  for the samples with an inhibitor concentration of 0.500 wt% may reflect the contribution from decay or termination of primary radicals.

As shown in Figs. 3–4 the most significant difference between pre-irradiation in air and argon in the present investigation is obtained for  $G_f$  in the inhibitor concentration range below 0.050 wt%. As mentioned in the introduction relatively stable alkylether radicals at  $\alpha$ -carbons are obtained in both atmospheres. As for other semicrystalline

polymers used in pre-irradiation grafting, like polyethylenes [34,36] and polyamides [5], the radicals generated throughout the bulk of the polymer, would only survive when trapped in the crystalline phase although with limited life times at ambient temperature [37]. Such radicals will migrate to the lamellae surfaces where they may initiate grafting of vinyl monomers diffusing into the pre-irradiated polymers [38,39]. In the amorphous phase above  $T_g$  the radicals rapidly decay by crosslinking or, when oxygen is present, by oxidation. The main differences in grafting rates and  $G_f$  as a result of pre-irradiation atmosphere, have been related to differences in crosslinking throughout the amorphous phase. This is readily observed for polyethylenes [34,36]. In the case of PCL, crosslinking in the amorphous phase upon irradiation under inert conditions is retarded since the probabilities for crosslinking and chain scission are about equal [24,40,41]. In order to form measurable gel contents by EB or  $\gamma$ -irradiation, doses of 20–26 Mrad have been reported [24,26]. Thus the dose range up to 10 Mrad used in the present investigation is far below the gel dose for PCL regardless of irradiation atmosphere. Consequently, the observed differences in  $G_f$  could not be related to crosslinking in the amorphous phase upon pre-irradiation in argon. In earlier investigations [24,26] for PCL irradiated

Table 4

Dose exponents of samples pre-irradiation in air or argon

Inhibitor concentration (wt%)	Pre-irradiation in air $a^{\text{air}}$ (a.u.)	Pre-irradiation in argon $a^{\text{argon}}$ (a.u.)
0.005	0.73	0.47
0.010	0.75	–
0.025	0.71	–
0.050	0.75	0.53
0.100	0.60	–
0.250	0.49	–
0.500	0.45	0.28



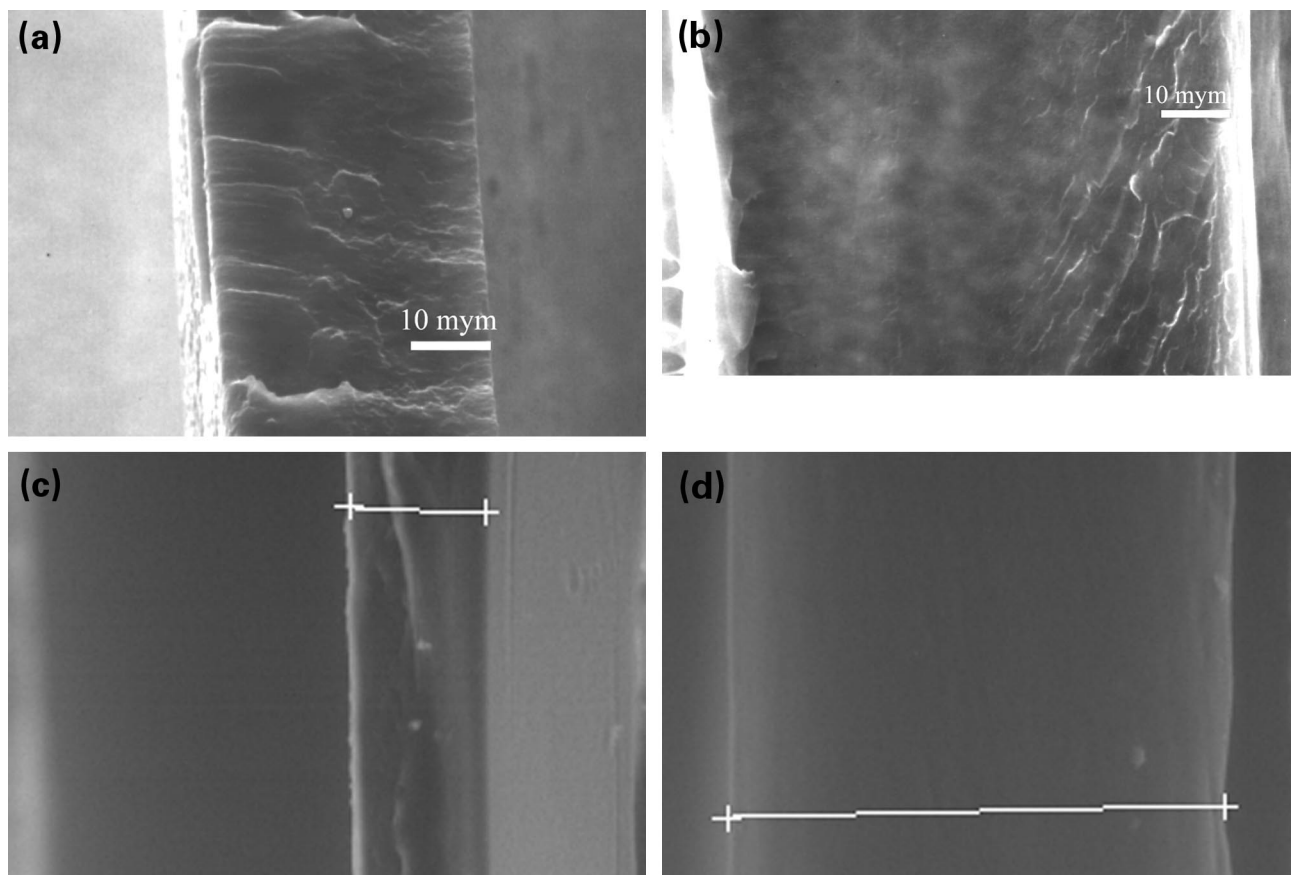


Fig. 7. Micrographs of P(CL-g-AAm) pre-irradiated in air: (a) (b) SEM and (c) (d) ESEM of cross sections, see Table 5.

by  $\gamma$ - or EB-irradiation under inert conditions it was concluded that crosslinking occurred between chain folds in the crystalline lamellae. Also chain scission and crosslinking were considered to occur, preferentially in the transient phase and at the crystallite surfaces. Similar results were obtained for polyethylenes [31] where it also has been found that the highest concentrations of radicals were trapped on the crystallite surfaces after migration from the interior of the crystallites [42,43]. Since oxygen will rapidly diffuse into the non-ordered regions under pre-irradiation in air, the initial amount of radicals in the amorphous phase and at the crystallite surfaces will be consumed by oxidation reactions. Only in the interior of the crystallites, where the diffusion of oxygen is much slower will trapped radicals remain. In a succeeding grafting step the differences between irradiation in air or argon would be related to differences in crosslinking localised to the surface zones of the crystallites and to the initial surface concentrations of radicals. Thus for PCL pre-irradiated in argon, a higher  $G_f$  would be explained by the higher initial concentration of radicals in crystallite surface regions. As seen from Tables 2 and 3 and visualised in Fig. 3a and b, this actually occurs for high concentrations of inhibitor concentrations, where the  $G_f$  and grafting rates are small. Under these conditions differences in radical concentration at the surfaces are more important than at higher grafting rates

when the crystallites are rapidly disintegrated. On the contrary, crosslinking between lamellae folds and in the intermediate phase will hinder monomer diffusion and expansion of the crystallite surface regions as grafting proceeds. This would be one factor favouring the higher  $G_f$  for pre-irradiation in air at low inhibitor concentrations. Also, as mentioned in the introduction, peroxy radicals are formed in addition to the alkylether radicals upon irradiation in air. If these would contribute to graft initiation they must be transformed into peroxides, which in turn, should give radicals by decomposition in a subsequent grafting step. In a recent study PCL seemed to give faster grafting rate with acrylic acid when pre-irradiated in air as compared to pre-irradiation in nitrogen [26]. However, within experimental error, there seemed to be no difference in  $G_f$ . Further, it was shown that PCL pre-irradiated from 2.5 to 10 Mrad under nitrogen lost all grafting reactivity within an hour after storage at ambient conditions. On the contrary the graft yield was found to increase with crystallinity when PCL was pre-irradiation grafted without intermittent exposure to air. In the present investigation, there is no clear indication of significant contribution from peroxide initiation. As seen in Figs. 3a and b and 4b, the considerably higher  $G_f$  for pre-irradiation in air below an inhibitor concentration of about 0.050 wt% is reversed above this concentration. Although all  $G_f$  values are small in this higher concentration

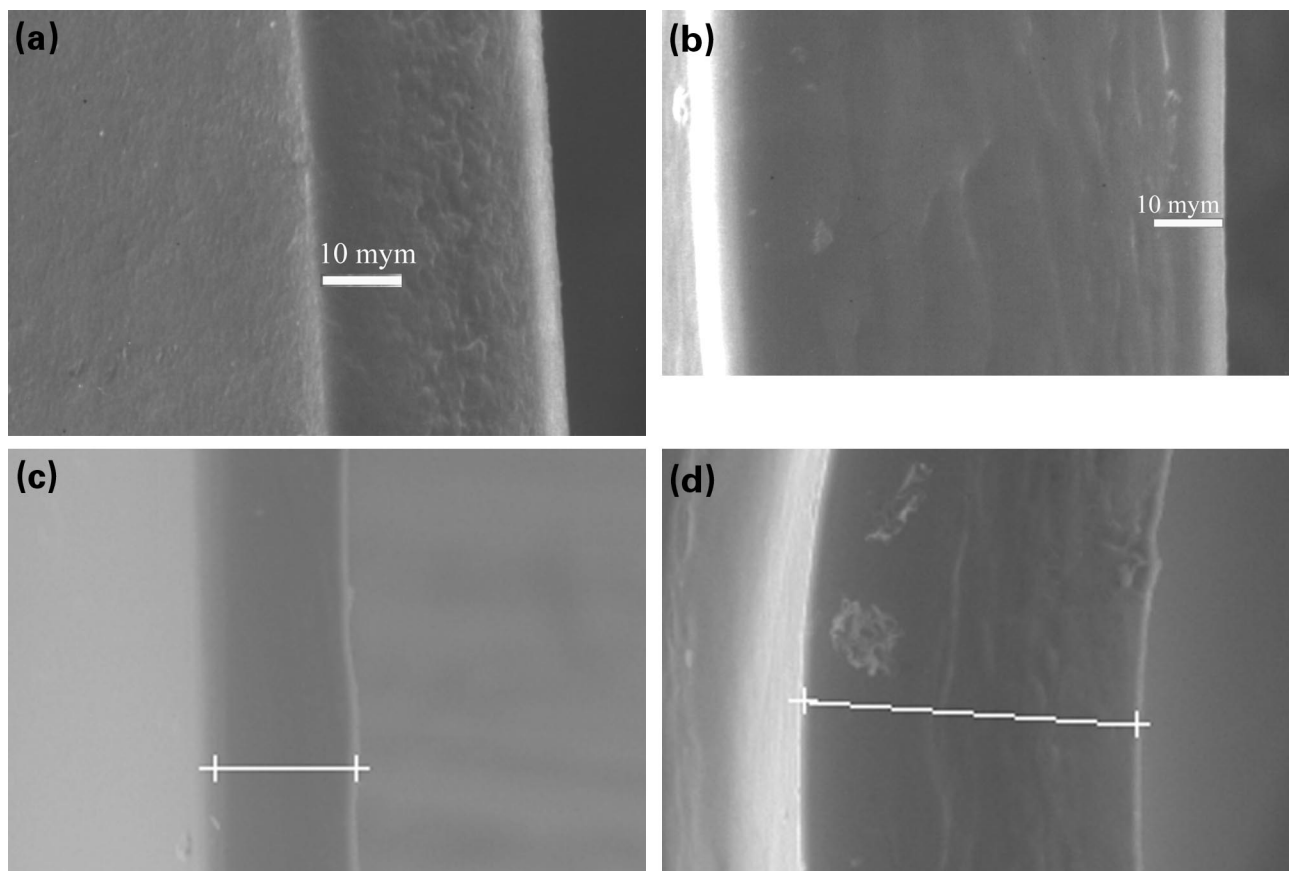


Fig. 8. Micrographes of P(CL-g-AAm) pre-irradiated in argon: (a) (b) SEM and (c) (d) ESEM of cross sections, see Table 5.

range the argon values are consistently higher for all doses, in spite of the fact that  $\text{Fe}^{2+}$  is a co-initiator with peroxides [34]. The peroxide radical observed for pre-irradiation in air [12] may rapidly decay to oxidation products other than peroxides, like carbonyls or hydroxylic groups, which has been observed for irradiated polyethylenes [9,39]. At the present stage, we conclude that the higher  $G_f$  data for pre-irradiation in air is due to the differences in crosslinking in the crystallite surface regions.

### 3.6. Expansion during grafting

In Figs. 7 and 8 the cross-sections of samples of P(CL-g-AAm) pre-irradiated in air or argon, respectively, in dry or swollen condition are shown. The micrographs represent the extreme points in concentration of inhibitor and dose and, hence, final graft yields.

The results of the thickness analysis—detected from Figs. 7 and 8—are compiled in Table 5.

As the concentration of inhibitor ( $[MS]$ ) is decreased,  $G_f$  is increased and the thickness, both in dry ( $t_{SEM}$ ) and swollen condition ( $t_{ESEM}$ ), is increased, as deduced from Table 5. The initial thickness of the PCL film is 30  $\mu\text{m}$ . Upon grafting, the thickness expands to about three times and to four times in the dry and swollen condition, respectively, for samples pre-irradiated in air. The maximum expansion for samples

pre-irradiated in argon is about three times for both measurements.

As seen in Fig. 9, the swelling of the lateral dimensions are almost identical for the air and argon samples, although there exists a weak tendency to lower expansion of the samples pre-irradiated in argon. The latter is emphasised in Fig. 9c: the curve approximation of the thickness in swollen condition is clearly lower for argon samples than that of air samples. As enlarged grafted specimens are obtained by variations in dose and inhibitor concentration, the initial shape is preserved. An isolated study showed that an initial triangular shape also generated a preserved final triangular shape in the final grafted state. Separate measurements have been performed to conclude whether the morphology is uniform over the entire specimen. DSC analysis yielded a uniform morphology since the crystallinity was almost constant at five different locations within the specimen investigated. Thus, the initial morphology is still present at increased graft yields and is represented in the entire specimen. The possible presence of crosslinking in the transient phase and at the crystallite surface zones of samples pre-irradiated in argon are probably the causes for the lower expansion in swelling, as compared to samples pre-irradiated in air. In Fig. 10 the ratio of the lateral dimensions ( $W/L$ ) as a function of graft yield for samples pre-irradiated in air or argon are displayed.

Table 5

Thickness of the films in dry condition ( $t_{SEM}$ ) and swollen condition ( $t_{ESEM}$ ), lateral dimension ( $L \times W$ ) and final graft yields ( $G_f$ ) for specific samples within the set as indicated

Atmosphere	Air		Argon	
	2.5	10	2.5	10
[MS] <sup>a</sup> = 0.500 wt%	$t_{SEM} = 34 \mu\text{m}$ (Fig. 7a) $t_{ESEM} = 33 \mu\text{m}$ (Fig. 7c) $L \times W = 23 \times 31 \text{ mm}^2$ $G_f = 74 \text{ wt}\%$	$t_{SEM} = 47 \mu\text{m}$ $t_{ESEM} = 50 \mu\text{m}$ $L \times W = 26 \times 34 \text{ mm}^2$ $G_f = 134 \text{ wt}\%$	$t_{SEM} = 31 \mu\text{m}$ (Fig. 8a) $t_{ESEM} = 34 \mu\text{m}$ (Fig. 8c) $L \times W = 23 \times 31 \text{ mm}^2$ $G_f = 92 \text{ wt}\%$	$t_{SEM} = 32 \mu\text{m}$ $t_{ESEM} = 43 \mu\text{m}$ $L \times W = 27 \times 34 \text{ mm}^2$ $G_f = 154 \text{ wt}\%$
[MS] <sup>a</sup> = 0.050 wt%	$t_{SEM} = 40 \mu\text{m}$ $t_{ESEM} = 55 \mu\text{m}$ $L \times W = 31 \times 37 \text{ mm}^2$ $G_f = 222 \text{ wt}\%$	$t_{SEM} = 60 \mu\text{m}$ $t_{ESEM} = 59 \mu\text{m}$ $L \times W = 49 \times 49 \text{ mm}^2$ $G_f = 587 \text{ wt}\%$	$t_{SEM} = 44 \mu\text{m}$ $t_{ESEM} = 39 \mu\text{m}$ $L \times W = 37 \times 39 \text{ mm}^2$ $G_f = 289 \text{ wt}\%$	$t_{SEM} = 47 \mu\text{m}$ $t_{ESEM} = 49 \mu\text{m}$ $L \times W = 44 \times 46 \text{ mm}^2$ $G_f = 518 \text{ wt}\%$
[MS] <sup>a</sup> = 0.005 wt%	$t_{SEM} = 76 \mu\text{m}$ $t_{ESEM} = 74 \mu\text{m}$  $L \times W = 61 \times 65 \text{ mm}^2$ $G_f = 1197 \text{ wt}\%$	$t_{SEM} = 80 \mu\text{m}$ (Fig. 7b) $t_{ESEM} = 121 \mu\text{m}$ (Fig. 7d)  $L \times W = 89 \times 95 \text{ mm}^2$ $G_f = 3436 \text{ wt}\%$	$t_{SEM} = 54 \mu\text{m}$ $t_{ESEM} = 73 \mu\text{m}$  $L \times W = 55 \times 56 \text{ mm}^2$ $G_f = 868 \text{ wt}\%$	$t_{SEM} = 74 \mu\text{m}$ (Fig. 8b) $t_{ESEM} = 81 \mu\text{m}$ (Fig. 8d)  $L \times W = 65 \times 72 \text{ mm}^2$ $G_f = 1403 \text{ wt}\%$

<sup>a</sup>MS = Mohr's salt.

References to Figs 7 and 8 in parenthesis.

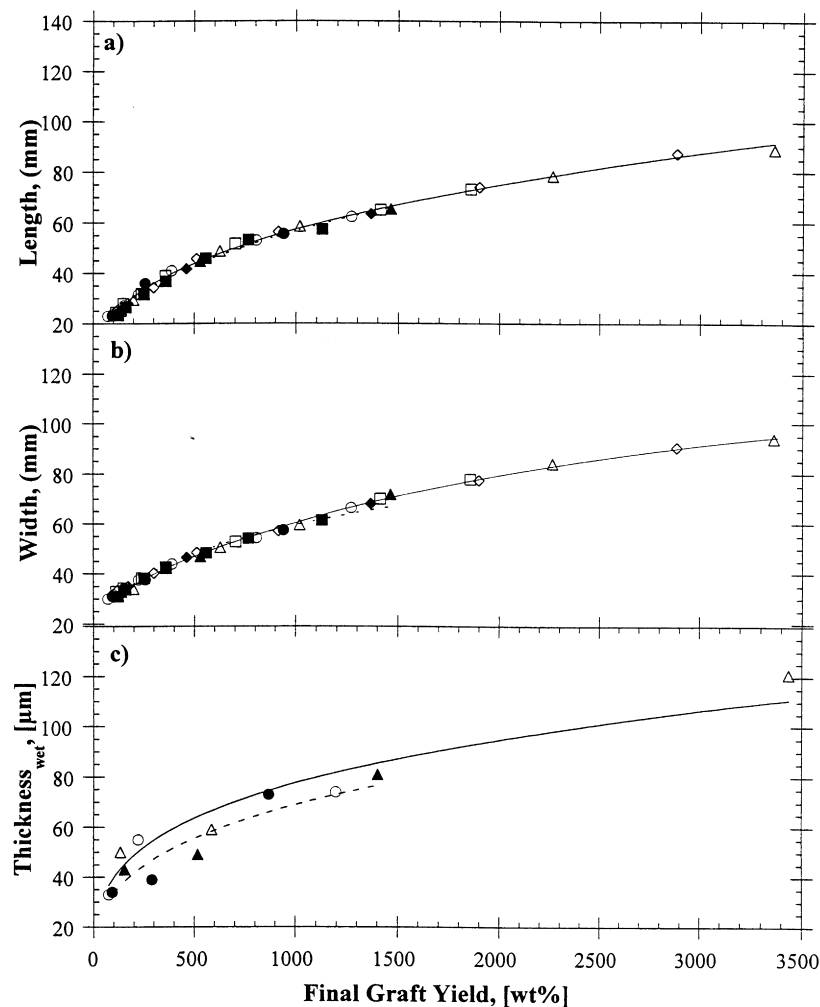


Fig. 9. Length, width and thickness in swollen condition as a function of final graft yield for P(CL-g-AAm) pre-irradiated in air (open symbols and straight lines) or argon (closed symbols and broken lines) to 2.5 Mrad (circles), 5 Mrad (boxes), 7.5 Mrad (diamonds) and 10 Mrad (triangles). Conditions as in Tables 2 and 3.

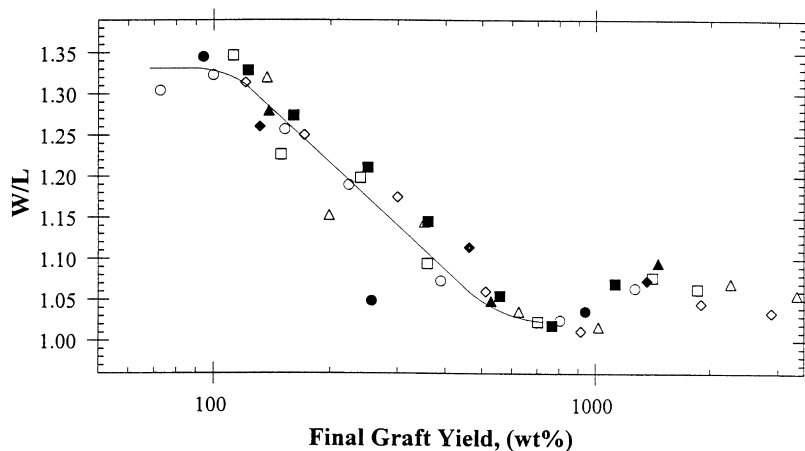


Fig. 10. The ratio of the lateral dimensions as a function of graft yield for P(CL-g-AAm) pre-irradiated in air (open symbols) or argon (closed symbols) to 2.5 Mrad (circles), 5 Mrad (boxes), 7.5 Mrad (diamonds) and 10 Mrad (triangles). Conditions as in Tables 2 and 3.

The ratio ( $W/L$ ) shows the effect the grafted chains have upon the orientation within the film. As the ( $W/L$ ) is altered to lower values orientation effects vanish and thus the morphology of the trunk polymer is transformed. The grafted chains disintegrate the original structure of the trunk polymer and create a mixed morphology, which is more uniform in all dimensions. The ratio ( $W/L$ ) as a function of  $G_f$  is similar for samples pre-irradiated in air or argon; samples pre-irradiated in argon have slightly higher values than samples pre-irradiated in air. Nevertheless, the trend, indicated by a curve approximation in Fig. 10, is regarded to be valid for both cases. The trend shows a constant ( $W/L$ ) value at a  $G_f$  below  $\sim 100$  wt% followed by a linear decrease as the  $G_f$  is increased. During the linear decrease of ( $W/L$ ) the initial biaxial morphology becomes disintegrated by the increased amount of grafted PAAM. At a  $G_f$  around 800 wt%, the ( $W/L$ ) has an almost constant value and the effect of the orientation has vanished.

#### 4. Conclusions

Final graft yields for air samples are much higher than those of argon samples at low inhibitor concentrations and doses ( $\geq 5$  Mrad) while argon samples have slightly higher final graft yields for inhibitor concentrations of 0.050 wt% and higher. Samples pre-irradiated in air and subsequently graft polymerised have higher degrees of crystallinity in the entire range of dose and concentration of inhibitor. The thickness of samples pre-irradiated in air had slightly higher values after swelling in water than those of samples pre-irradiated in argon. These properties are attributed to crosslinking localised in the transient phase and at crystallite surface zones for samples pre-irradiated in argon.

#### References

- [1] Dessouki AM, Hegazy EA, El-Assy NB, El-Boohy HA. *Radiat Phys Chem* 1986;27:431.
- [2] Hegazy E-SA, Dessouki AM, El-Assy NB, El-Sawy NM, El-Ghaffar MAA. *Polym Sci A: Polym Chem* 1992;30:1969.
- [3] Ellinghorst G, Fuehrer J, Vierkotten D. *Radiat Phys Chem* 1981;18:889.
- [4] Fuehrer J, Ellinghorst G. *Die Ang Makromol Chem* 1981;93:175.
- [5] Haruvy Y, Rajbenbach LA, Jagur-Grodzinski J. *Appl Polym Sci* 1982;27:2711.
- [6] Harada J, Chern RT, Stannett VT. *Polym Prepr* 1990;31:370.
- [7] Postnikov VA, Lukin NJu, Maslov BV, Platé NA. *Polym Bull* 1980;3:75.
- [8] Mori K, Koshiishi K, Masuhara K. *Appl Polym Sci* 1991;43:553.
- [9] Ohnishi S-I, Sugimoto S-I, Nitta I. *J Polym Sci A* 1963;1:605.
- [10] Lawton EJ, Balwit JS, Powell RS. *Polym Sci* 1958;32:257.
- [11] Dole M. In: Dole M, editor. *The radiation chemistry of macromolecules*, 2. New York: Academic, 1973. p. 263.
- [12] Ohrlander M, Erickson R, Palmgren R, Wirsén A, Albertsson A-C. *Polymer* Accepted for publication.
- [13] Koleske JV, Lundberg RD. *J Polym Sci A-2* 1969;7:795.
- [14] Chatani Y, Ôkita Y, Tadokoro H, Yamashita Y. *Polym J* 1970;1:555.
- [15] Wunderlich B, Baur H. *Adv Polym Sci* 1970;7:151.
- [16] Crescenzi V, Manzini G, Calzolari G, Borri C. *Eur Polym J* 1972;8:449.
- [17] Wirsén A, Ohrlander M, Albertsson A-C. *Biomaterials* 1996;17:1881.
- [18] Wirsén A. Thesis, KTH, Stockholm, 1995.
- [19] Ohrlander M, Wirsén A, Albertsson A-C. *J Polym Sci A: Polym Chem* 1999;37:1643.
- [20] Martinez-Salazar J, Gonzalez-Ortega JC, Baltá-Calleja FJ. *Anal Fis* 1977;73:244.
- [21] Baltá-Calleja FJ, Vonk CG. 1. X-ray scattering of synthetic polymers, Amsterdam: Elsevier, 1989. p. 5.
- [22] Kakudo M, Kasai N. X-ray diffraction of polymers, Amsterdam: Elsevier, 1972. pp. 282 see also p. 358, 400, 436, 446.
- [23] Janigová I, Csomorová K, Stillkammerová M, Barton J. *Macromol Chem Phys* 1994;195:3609.
- [24] Narkis M, Sibony-Chaouat S, Siegmann A, Shkolnik S, Bell JP. *Polymer* 1985;26:50.
- [25] Phillips PJ, Rensch GJ, Taylor KD. *Polym Sci B: Polym Phys* 1987;25:1725.
- [26] Södergård A. *Polym Sci A: Polym Chem* 1998;36:1805.

- [27] Premnath V, Bellare A, Merrill EW, Jasty M, Harris WH. *Polymer* 1999;40:2215.
- [28] Salovey R, Shinde A. *Polym Prepr* 1985;26:118.
- [29] Aslanian VM, Vardanian VI, Avetisian MH, Felekian SS, Ayvasian SR. *Polymer* 1987;28:755.
- [30] Salovey R, Bassett DC. *Appl Phys* 1964;35:3216.
- [31] Kashiwabara H, Shimada S, Hori Y. *Radiat Phys Chem* 1991;37:43.
- [32] Hoffman JD, Miller RL, Marand H, Roitman DB. *Macromolecules* 1992;25:2221.
- [33] Wirsén A, Albertson A-C, Albertsson. *J Polym Sci A: Polym Chem* 1995;33:2049.
- [34] Ishigaki I, Sugo T, Takayama T, Okada T, Okamoto J, Machi S. *Appl Polym Sci* 1982;27:1043.
- [35] Ishigaki I, Sugo T, Takayama T, Okada T, Okamoto J, Machi S. *Appl Polym Sci* 1982;27:1033.
- [36] Wirsén A, Albertsson A-C. *J Polym Sci A: Polym Chem* 1995;33:2039.
- [37] Wirsén A, Lindberg T, Albertsson A-C. *Polymer* 1996;37:761.
- [38] Seguchi T, Tamura N. *Polym Sci: Polym Chem* 1974;12:1671.
- [39] Uezu K, Saito K, Furusaki S, Sugo T, Ishigaki I. *Radiat Phys Chem* 1992;40:31.
- [40] Gandhi K, Kriz D, Salovey R, Narkis M, Wallerstein R. *Polym Engng Sci* 1988;28:1484.
- [41] Darwis D, Mitomo H, Enjoji T, Yoshii F, Makuuchi K. *Appl Polym Sci* 1998;68:581.
- [42] Shimada S, Maeda M, Hori Y, Kashiwabara H. *Polymer* 1977;18:19.
- [43] Shimada S, Hori Y, Kashiwabara H. *Polymer* 1977;18:25.